Retinoic Acid Maintains Function of Neural Crest–Derived Ocular and Craniofacial Structures in Adult Zebrafish

Bahaar Chawla, William Swain, Antionette L. Williams, and Brenda L. Bohnsack

Department of Ophthalmology and Visual Sciences, Kellogg Eye Center, University of Michigan, Ann Arbor, Michigan, United States

Correspondence: Brenda L. Bohnsack, Department of Ophthalmology and Visual Sciences, Kellogg Eye Center, University of Michigan, 1000 Wall Street, Ann Arbor, MI 48105, USA;
brendabo@med.umich.edu.

Submitted: August 21, 2017
Accepted: February 16, 2018

Citation: Chawla B, Swain W, Williams AL, Bohnsack BL. Retinoic acid maintains function of neural crest–derived ocular and craniofacial structures in adult zebrafish. *Invest Ophthalmol Vis Sci*. 2018;59:1924–1935. https://doi.org/10.1167/iovs.17-22845

Purpose. Retinoic acid (RA) is required for embryonic formation of the anterior segment of the eye and craniofacial structures. The present study further investigated the role of RA in maintaining the function of these neural crest–derived structures in adult zebrafish.

Methods. Morphology and histology were analyzed by using live imaging, methylacrylate sections, and TUNEL assay. Functional analysis of vision and aqueous humor outflow were assayed with real-time imaging.

Results. Both decreased and increased RA signaling altered craniofacial and ocular structures in adult zebrafish. Exogenous treatment with all-trans RA for 5 days resulted in a prognathic jaw, while inhibition of endogenous RA synthesis through treatment with 4-diethylaminobenzaldehyde (DEAB) decreased head height. In adult eyes, RA activity was localized to the retinal pigment epithelium, photoreceptors, outer plexiform layer, inner plexiform layer, iris stroma, and ventral canalicular network. Exogenous RA increased apoptosis in the iris stroma and canalicular network in the ventral iridocorneal angle, resulting in the loss of these structures and decreased aqueous outflow. DEAB, which decreased RA activity throughout the eye, induced widespread apoptosis, resulting in corneal edema, cataracts, retinal atrophy, and loss of iridocorneal angle structures. DEAB-treated fish were blind with no optokinetic response and no aqueous outflow from the anterior chamber.

Conclusions. Tight control of RA levels is required for normal structure and function of the adult anterior segment. These studies demonstrated that RA plays an important role in maintaining ocular and craniofacial structures in adult zebrafish.

Keywords: retinoic acid, vitamin A, zebrafish, neural crest, aqueous humor outflow

Vitamin A (retinol) is an essential nutrient, as its derivatives are required for embryonic development and the function of postnatal tissues.[1–4] Retinol is the precursor of retinaldehyde (retinal), which can then be converted into retinoic acid (RA).[5,6] The series of enzymatic reactions that mediate the synthesis and degradation of retinal and RA are tightly regulated, as both the deficiency and excess of these factors play a role in disease pathogenesis.[6]

RA is a key signal in the cranial neural crest, a transient population of stem cells that is critical for craniofacial and ocular development.[7–13] The cranial neural crest gives rise to the bone, cartilage, and peripheral nerves of the midface and frontal regions. In addition, this stem cell population contributes to the formation of the anterior segment structures of the eye, including the cornea, iris, trabecular meshwork, ciliary body, and sclera.[14–16] RA is also important in postnatal tissues. Vitamin A deficiency, reflecting poor diet or malabsorption, is characterized by nyctalopia (night blindness), xerophthalmia (decreased tear production), and keratomalacia (corneal thinning and opacification).[17,18] In bone, RA maintains mineral density, as both increased and decreased levels are associated with increased risk of fractures.[19–23] RA regulates the balance between osteoblast and osteoclast differentiation and activity; however, the specific effect is dependent on the bone type and location.[24]

RA derivatives are common therapeutic agents for acne vulgaris and certain types of cancer.[25–28] However, the effects of long-term exposure to RA on neural crest–derived craniofacial and ocular structures have not been studied. The current studies investigated the continued need for the tight control of RA signaling within neural crest–derived adult craniofacial structures and the eye. Using adult zebrafish, we determined the functional, anatomic, and histologic effects of increased or decreased RA. Interestingly, the anterior segment and regulation of aqueous outflow from the eye were highly sensitive to alterations in RA, suggesting a role for RA in maintaining these structures.

Materials and Methods

Animal Care/Animal Strains

Wild-type 10- to 14-month-old AB male and female adult zebrafish (*Danio rerio*) were raised in a breeding colony under a 14-hour light/10-hour dark cycle as previously described.[14,15,29–31] Both wild-type and the Tg(*rare:mCherry*) strain[15] were crossed into the Casper (*nacre*$^{-/-}$, *roy*$^{-/-}$) background to decrease autofluorescence and pigment. Animal protocols were performed in accordance with the guidelines for the humane treatment of laboratory animals established by the University of Michigan Committee on the Use and Care of Animals (IACUC, protocol No. 10205) and the ARVO Statement for the Use of Animals in Ophthalmic and Vision Research.

Pharmacologic Treatments

All-trans RA (Sigma-Aldrich Corp., St. Louis, MO, USA), 4-diethylaminobenzaldehyde (DEAB; Sigma-Aldrich Corp.), the retinoic acid receptor (RAR)α antagonist BMS195614 (Tocris Biosciences, Avonmouth, Bristol, UK), the RARβ antagonist LE135 (Tocris Biosciences), and the RARγ antagonist MM11253 (Tocris Biosciences) were diluted to 1000× treatment concentrations in dimethylsulfoxide (DMSO; Sigma-Aldrich Corp.) and added into reverse osmosis system fish water at 1× final concentrations. Dose curves were conducted for each pharmacologic treatment (10, 25, and 100 nM RA; 5, 10, and 15 μM DEAB; 1 and 10 μM BMS195614; 0.1, 1, and 10 μM LE135; and 0.1, 1, and 10 nM MM11253), and the final concentrations were selected by the LD50 and consistency of phenotype (data not shown). The final concentrations were 100 nM RA, 10 μM DEAB, 1 μM BMS195614, 1 μM LE135, and 10 nM MM11253.

For all experiments, an equal number of male and female, age-matched (10–14 month old) adult zebrafish were treated with 0.1% DMSO (control), 100 nM RA, 10 μM DEAB, 1 μM BMS195614, 1 μM LE135, and 10 nM MM11253 in 1 L reverse osmosis system fish water. For each experiment, four to six fish per treatment condition were used. Treatments were refreshed daily. Both treated and untreated fish were maintained in dark conditions owing to the light sensitivity of the reagents and were fasted through the duration of the experiment. The fish were analyzed and harvested after 2 or 5 days of treatment as indicated.

Live Imaging

Following 5 days of pharmacologic treatment, the fish were anesthetized in 0.05% tricaine methanesulfonate (MS-222; Sigma Aldrich) and mounted in 3% methylcellulose (Sigma Aldrich) in reverse osmosis system fish water. The fish were imaged by using a Leica M205FA combi-scope (Leica Microsystems CMS GmbH, Wetzler, Germany). Images were obtained by using a Leica DFC290 camera and Leica Application Suite (LAS). The images were processed and analyzed by using LAS (Leica) and Adobe Photoshop (San Jose, CA, USA). Lateral images that captured the full head height and the length from the jaw to the gills were obtained. The images shown are representative of all experiments.

Measurements of the craniofacial regions of four to six fish, including the anterior to posterior corneal diameter (Fig. 1A, yellow line), head height at the gills (Fig. 1A, red line), jaw length (Fig. 1A, green line), and distance of the gills from the eye (Fig. 1A, blue line) were obtained with Adobe Photoshop. The data were statistically analyzed by using ANOVA with Tukey's post hoc analysis, and $P < 0.05$ was considered statistically significant.

Optokinetic Reflex Test

Adult zebrafish were anesthetized in 0.05% MS-222, immobilized in foam and 3% methylcellulose, and placed inside a transparent cylinder containing fresh reverse osmosis system fish water. The fish, which were then placed inside a hollow rotating drum with vertical alternating white and black stripes, were recovered from the anesthesia for 5 minutes before testing. Testing lasted 3 minutes and comprised 15-second intervals of no movement or the clockwise or counterclockwise movement of the drum (Fig. 2). The fish were scored by their ability to accurately track the applied changes in drum movement. Five fish per group were tested before pharmacologic treatment and at 5 days post treatment. The data were statistically analyzed by using ANOVA with Tukey's post hoc analysis, and $P < 0.05$ was considered statistically significant.

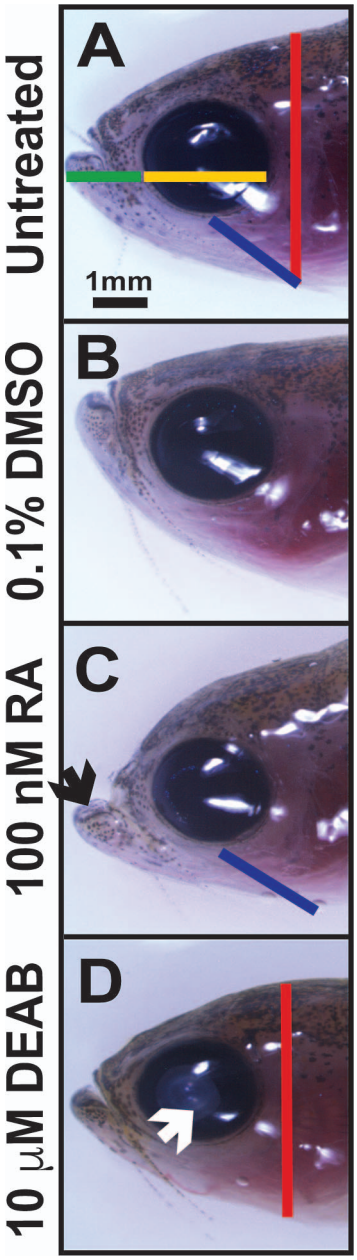

Figure 1. Alterations in RA affect craniofacial structures. Treatment of adult zebrafish with 100 nM RA (**C**) for 5 days caused a prognathic jaw (*black arrow*) and increased distance from the eye to the gill (*blue line*) as compared to untreated (**A**) and 0.1% DMSO control–treated (**B**) fish. Inhibition of RA synthesis through treatment with the pan-aldehyde dehydrogenase inhibitor DEAB (10 μM) for 5 days (**D**) decreased the height of the head (*red line*) and caused cataract formation (*white arrow*). Treatment with RA or DEAB did not affect the jaw length (*green line*, [**A**]) or horizontal (anterior to posterior) diameter of the cornea (*yellow line*, [**A**]).

Zebrafish Ocular Histology

Adult zebrafish were decapitated, and the heads were fixed in 4% paraformaldehyde overnight followed by decalcification in 10% ethylenediaminetetraacetic acid (EDTA) for 5 days at 4°C. The heads were refixed in 2% paraformaldehyde/1.5% glutaraldehyde, followed by embedding in methylacrylate. The blocks were sectioned at 5 μm. The sections were stained with Lee's stain, coverslipped, and subsequently imaged.

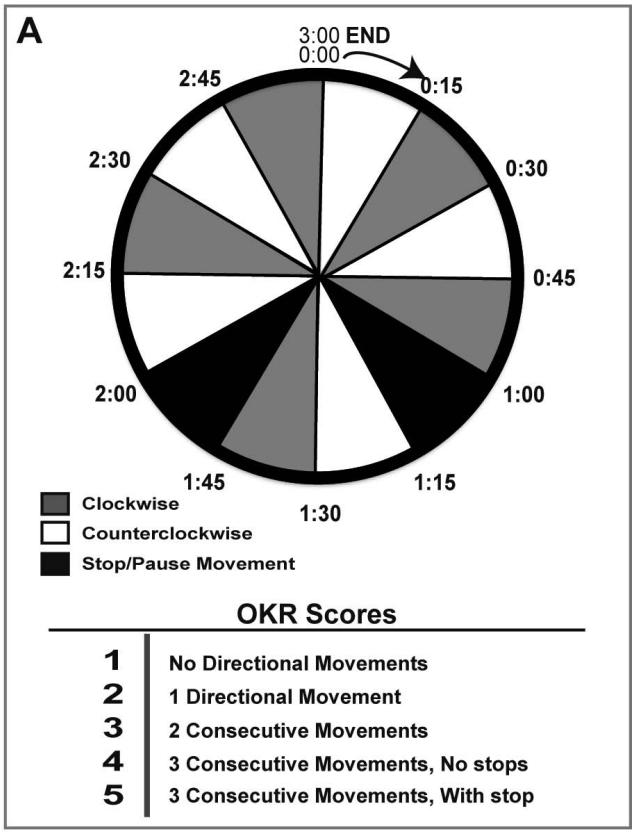

Figure 2. RA is required for visual function. Optokinetic (OKR) reflex testing was performed with a 3-minute protocol that included directional changes with stops (**A**). The fish were subjected to 15-second intervals of clockwise or counterclockwise movements of the optokinetic drum. In addition, two 15-second intervals were included in which there was no movement of the drum. Fish were scored from 1 to 5 by the ability to correctly track the drum movement. All fish were tested before treatment and showed an average score of 4.7 ± 0.3. Treatment with 100 nM RA for 5 days did not significantly decrease the optokinetic reflex score as compared to untreated or 0.1% DMSO control–treated fish (**B**). Fish treated with 10 μM DEAB for 5 days were not able to detect any directional movement of the optokinetic drum and scored significantly ($P < 0.02$) worse than untreated or 0.1% DMSO control–treated fish.

Immunostaining and TUNEL Assay

Adult zebrafish were decapitated, and the heads were fixed in 4% paraformaldehyde overnight followed by decalcification in 5% trichloroacetic acid at 4°C for 48 hours. The heads were cryoprotected in successive sucrose solutions, embedded in optimal cutting temperature (OCT) mounting medium, and cryosectioned at 10 μm.

For immunostaining detection of mCherry signal in Tg(*rare:mCherry)* fish, the sections were fixed in ice-cold acetone, washed in phosphate-buffered solution (PBS), and then blocked in 10% normal goat serum in 0.1% Tween 20 in PBS. The sections were incubated with rabbit anti-mCherry (1:500; Abcam, Cambridge, MA, USA) overnight at 4°C, washed in PBS, and then incubated with goat anti-rabbit conjugated with Alexa Fluor 647 (1:500; Thermo Fisher Scientific, Waltham, MA, USA). Sections were costained with DAPI and coverslipped, followed by imaging by using a DM6000B upright microscope (Leica) equipped with a DFC500 camera (Leica). The images were processed and analyzed by using Adobe Photoshop, LAS X (Leica), and/or LAS AF6000 software (Leica). Fluorescence intensity was measured in three consecutive sections from four to six fish per treatment group by using ImageJ (http://imagej.nih.gov/ij/; provided in the public domain by the National Institutes of Health, Bethesda, MD, USA). The data were statistically analyzed by using ANOVA with Tukey's post hoc analysis, and $P < 0.05$ was considered statistically significant.

TUNEL assay was performed by using standard protocols and as previously described.[15,32] Briefly, apoptotic cells were detected through the TdT (Roche, Indianapolis, IN, USA) mediated incorporation of digoxigenin-labeled deoxyuridine triphosphate (Roche). Sheep anti-digoxigenin conjugated to rhodamine (Roche) was used to detect the TUNEL signal. Sections were costained with DAPI and coverslipped, followed by imaging as described above. The number of TUNEL-positive cells and total number of cells, as demarcated by DAPI staining, within the eye were counted. The percentage of apoptotic cells was calculated in three consecutive sections of the eyes from four to six fish per treatment group. The data were statistically analyzed by using ANOVA with Tukey's post hoc analysis, and $P < 0.05$ was considered statistically significant.

Aqueous Outflow Tract Visualization

Zebrafish were anesthetized in 0.05% MS-222 in fish water and immobilized in 3% methylcellulose under the Leica M205FA combi-scope (described above). Dextran-conjugated Texas Red fluorescent dye (0.05 μL of 5 mM; Thermo Fisher Scientific) was injected into the anterior chamber by using a capillary needle as previously described.[33] Images were captured immediately after injection and at 20-second intervals for 15 minutes. Fresh 0.01% MS-222 solution was periodically added to maintain anesthesia. The images were processed in Adobe Photoshop and sewn together to create time-lapse movies using iMovie (Apple, Cupertino, CA, USA). Fluorescence intensity was measured in four fish per treatment group by using ImageJ at time of injection and after 5, 10, and 15 minutes. The fluorescence intensity for each fish was normalized to the amount measured at time of injection. The data were statistically analyzed by using Student's *t*-test and $P < 0.05$ was considered statistically significant.

Quantitative Real-Time RT-PCR Assay (qRT-PCR)

Total RNA was extracted from adult zebrafish eyes by using the RNeasy mini kit (Qiagen, Hilden, Germany), and reverse transcription was performed by using the Superscript IV reverse transcriptase (Thermo Fisher Scientific) according to the manufacturer's instructions. Real-time PCR experiments were performed by using the CFX96 Touch Real-Time Detection System (Bio-Rad, Hercules, CA, USA), and Power SYBR Green PCR Master Mix (Thermo Fisher Scientific). The

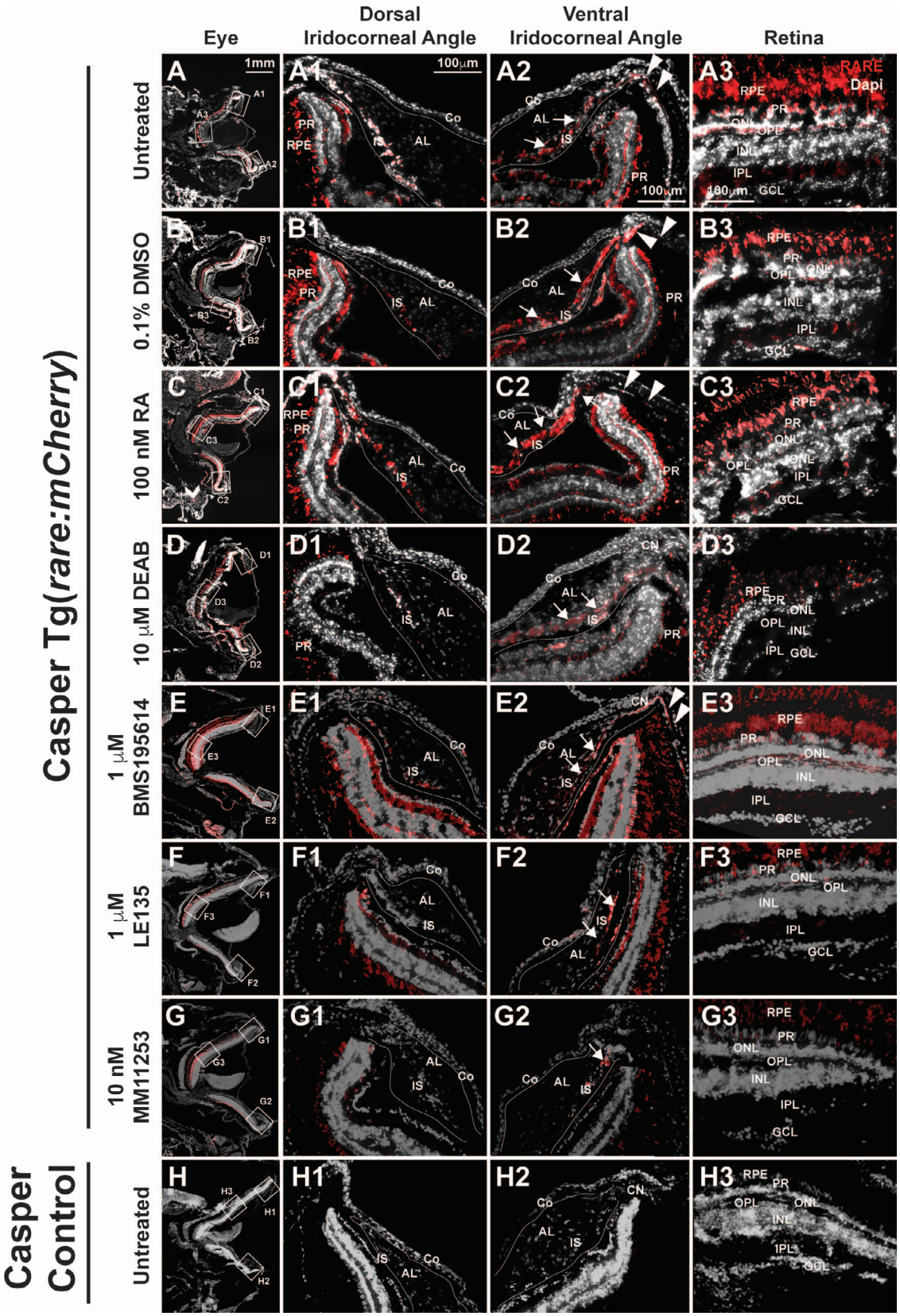

Figure 3. RA activity is in the retina and iridocorneal angles in the adult eye. In Casper Tg(*rare:mCherry*) adult zebrafish, RA activity was predominantly in the PRs and RPE in the adult eye of untreated (**A**, **A3**) and 0.1% DMSO control–treated (**B**, **B3**) fish. RA was also found in the OPL and IPL (**A3**, **B3**) in the retina. In the dorsal iridocorneal angle of untreated and control-treated eyes (**A1**, **B1**), RA activity was in the IS. In the ventral iridocorneal angle of untreated and control-treated eyes (**A2**, **B2**), RA was found in IS, the canalicular network that was between the iris and annular ligament (*arrows*), and the angular aqueous plexus (*arrowheads*). There was no detectable RA activity in the cornea (Co) in this reporter line.

Investigative Ophthalmology & Visual Science

Treatment with 100 nM RA for 5 days (**C**) increased RA activity in the IS in the dorsal (**C1**) and ventral (**C2**) angles and in the ventral canalicular network (*arrows*, [**C2**]), but not in the retina (**C3**). Treatment with 10 μM DEAB for 5 days (**D**) decreased RA activity throughout the eye including in the dorsal (**D1**) and ventral (**D2**) angles and in the retina (**D3**). Treatment with the RARα-specific antagonist BMS195614 (1 μM) for 5 days did not alter RA activity within the eye (**E**, **E1**, **E2**, **E3**). Treatment with the RARβ antagonist LE135 (1 μM, **F**) for 5 days showed mildly decreased RA activity in the retina in the PRs, OPL, and IPL (**F3**), but no change in the dorsal (**F1**) or ventral (**F2**) angles. Inhibition of RARγ with the specific antagonist MM11253 (10 nM) decreased RA throughout the eye (**G**), including in the angles (**G1**, **G2**) and retina (**G3**). Control Casper fish, which lack the transgene, showed minimal to no fluorescence in the eye (**H**, **H1**, **H2**, **H3**). AL, annular ligament; GCL, ganglion cell layer; INL, inner nuclear layer; ONL outer nuclear layer.

following PCR program was used: 95°C for 10 minutes, followed by 40 cycles at 95°C for 15 seconds and 60°C for 60 seconds. A melting curve analysis was applied to assess the specificity of the amplified PCR products. The PCR primer sequences are listed in Supplementary Table S1. The amount of each target gene was quantified by the comparative C_T method, using β-actin as the normalization control.

Results

RA Regulates Morphology of Adult Craniofacial Structures

The effects of altering RA levels on craniofacial structures were analyzed through live imaging before treatment and subsequently after 5 days of exposure to 0.1% DMSO control (Fig. 1B), 100 nM RA (Fig. 1C), or 10 μM DEAB (Fig. 1D). Treatment with DMSO (Fig. 1B) did not affect craniofacial structures as compared to untreated animals (Fig. 1A). Treatment with exogenous RA caused a prognathic jaw (Fig. 1C, black arrow) and significantly increased the distance from the eye to the gill (Fig 1C, blue line; Supplementary Fig. S1). Inhibition of RA synthesis via treatment with the pan–aldehyde dehydrogenase inhibitor DEAB caused cataract formation (Fig. 1D, white arrow) and significantly decreased head height (Fig. 1D, red line; Supplementary Fig. S1). Neither RA nor DEAB treatment significantly altered the anterior to posterior corneal diameter (Fig. 1A, yellow line; Supplementary Fig. S1) or the distance from the jaw to the eye (Fig. 1A, green line; Supplementary Fig. S1). Thus, changes in RA levels altered some dimensions of craniofacial structures after treatment for 5 days.

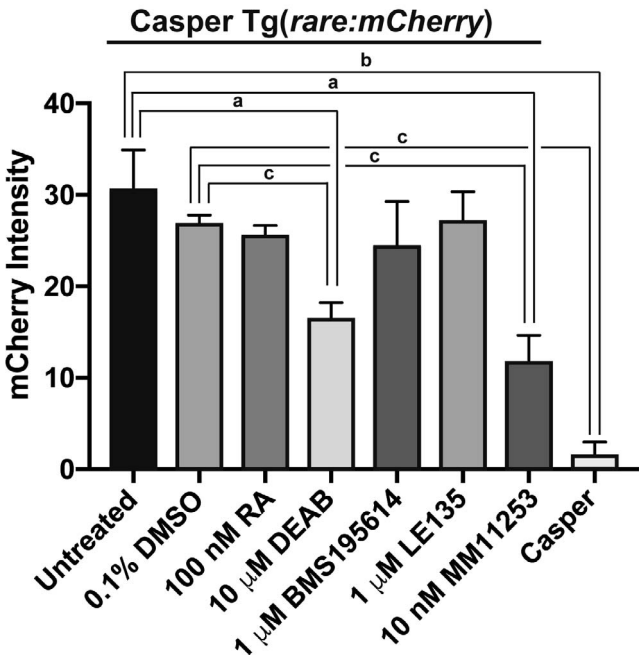

Figure 4. RARγ mediates RA activity in the adult zebrafish eye. Quantitative measurement of fluorescence intensity in eyes of Casper Tg(*rare:mCherry*) fish showed that inhibition of RA synthesis by 10 μM DEAB (16.5 ± 1.7) or treatment with the RARγ antagonist MM11253 at 10 nM (11.9 ± 2.7) significantly decreased mCherry signal as compared to untreated (30.5 ± 4.4) or 0.1% DMSO control–treated fish (26.9 ±1.0). Treatment with 100 nM RA (25.5 ± 1.1), 1 μM BMS195614 (24.4 ± 4.9), or 1 μM LE135 (27.3 ± 3.1) did not significantly alter mCherry signal intensity. There was minimal to no fluorescence signal in Casper fish, which do not carry the transgene (1.5 ± 1.5). (**a**) $P < 0.01$. (**b**) $P < 0.001$. (**c**) $P < 0.0001$.

Alterations in RA Reduced Visual Function

Changes in visual function resulting from exposure to RA or DEAB were analyzed by examining the optokinetic reflex, and the fish were scored (1 to 5) by the ability to correctly and accurately track drum movement (Fig. 2A). The fish were tested before and after 5 days of treatment. Before treatment, the average score of all animals was 4.7 ± 0.3 (Supplementary Video S1). After 5 days, untreated (Supplementary Video S2) and 0.1% DMSO control-treated fish (Supplementary Video S3) exhibited appropriate optokinetic reflexes and scored 5.0 ± 0.1 and 4.5 ± 0.7, respectively (Fig. 2B). Fish treated with 100 nM RA for 5 days showed some difficulty in continuously following more than two movements of the rotating drum (Supplementary Video S4); however, the posttreatment score (3.5 ± 0.7, $P = 0.3$) was not significantly decreased as compared to pretreatment (Fig. 2B). Not surprisingly, 10 μM DEAB impaired visual function, such that after 5 days of treatment, the fish were unable to track any drum movement (Fig. 2B; Supplementary Video S5) and scored significantly worse than untreated and control fish ($P = 0.02$). These studies demonstrated that the inhibition of RA synthesis decreased visual function in adult zebrafish.

Alterations in RA Activity Affect Ocular Histology

Given the effects on visual function, the activity of RA at the tissue level was analyzed in the eyes of adult transgenic fish expressing mCherry in cells with RA activity (Casper Tg(*rare:mCherry*); Fig. 3). Immunostaining for mCherry demonstrated endogenous RA activity in the retinal pigment epithelium (RPE), photoreceptors (PRs), outer plexiform layer (OPL), and inner plexiform layer (IPL) in untreated (Figs. 3, 3A3) and DMSO control–treated (Figs. 3B, 3B3) fish. In the anterior segment, RA was in the iris stroma (IS) in untreated (Figs. 3A1, 3A2) and DMSO control–treated (Figs. 3B1, 3B2) fish. RA was also present in the aqueous outflow tract of the adult zebrafish eye, which consists of the ventral canalicular network (Figs. 3A2, 3B2, arrows) and angular aqueous plexus (Figs. 3A2, 3B2, arrowheads). There was no difference in fluorescence intensity (Fig. 4) within the eyes of untreated (30.5 ± 4.4) or DMSO control–treated (26.9 ± 1.0) fish. Casper fish, which lacked the rare-mCherry transgene (Figs. 3H, 3H1, 3H2, 3H3), showed minimal to no fluorescence (1.5 ± 1.5; Fig. 4) as compared to untreated ($P < 0.001$) and DMSO control–treated ($P < 0.0001$) fish.

Investigative Ophthalmology & Visual Science

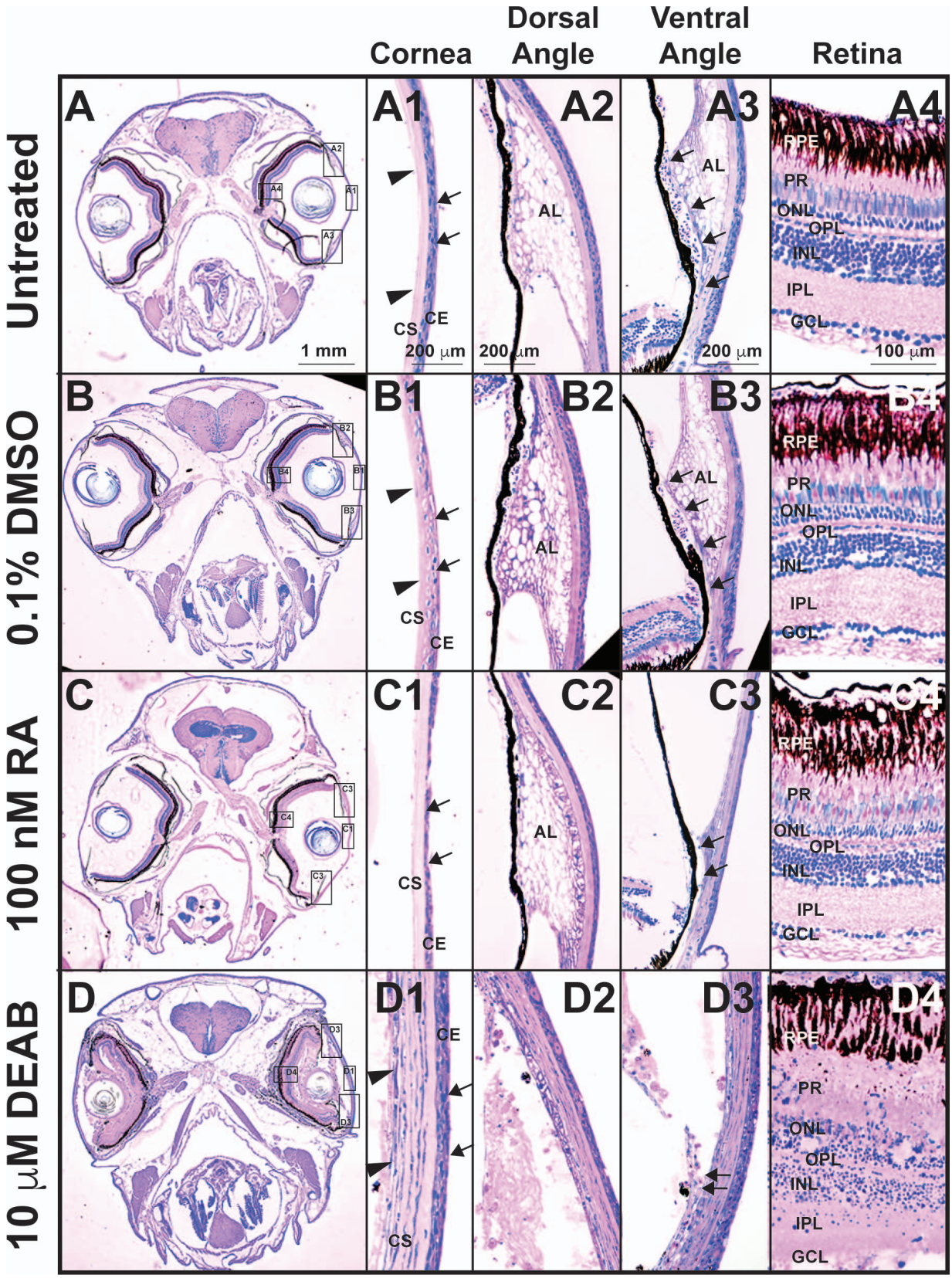

Figure 5. Tight control of RA levels is required for maintaining ocular structures. Methylacrylate sections of adult zebrafish treated with 100 nM RA for 5 days showed that exogenous RA decreased corneal epithelial cellularity (*arrows*, [**C**, **C1**]) as compared to untreated (**A**, **A1**) and DMSO control–treated (**B**, **B1**) fish. In the ventral iridocorneal angle (**C3**), RA also caused decreased iris stromal cellularity (**C3**) and loss of the webbed appearance of the AL and the ventral canalicular network (*arrows*, [**C3**]) compared to untreated (**A3**) and DMSO control-treated (**B3**) fish. The structures in the dorsal iridocorneal angle (**C2**) and retina (**C4**) were not affected by exogenous RA as compared to untreated (**A2**, **A4**) and DMSO control–treated (**B2**, **B4**) fish. Treatment with 10 μM DEAB for 5 days caused corneal stromal (*arrowheads*, [**D**, **D1**]) and epithelial (*arrows*, [**D1**]) edema and loss of architecture in the dorsal (**D2**) and ventral (**D3**) iridocorneal angles. DEAB also disrupted retinal structure, which included loss of PRs (**D4**) and ganglion cells (GCL, **D4**). AL, annular ligament; Co, cornea; GCL, ganglion cell layer; INL, inner nuclear layer; ONL outer nuclear layer.

Investigative Ophthalmology & Visual Science

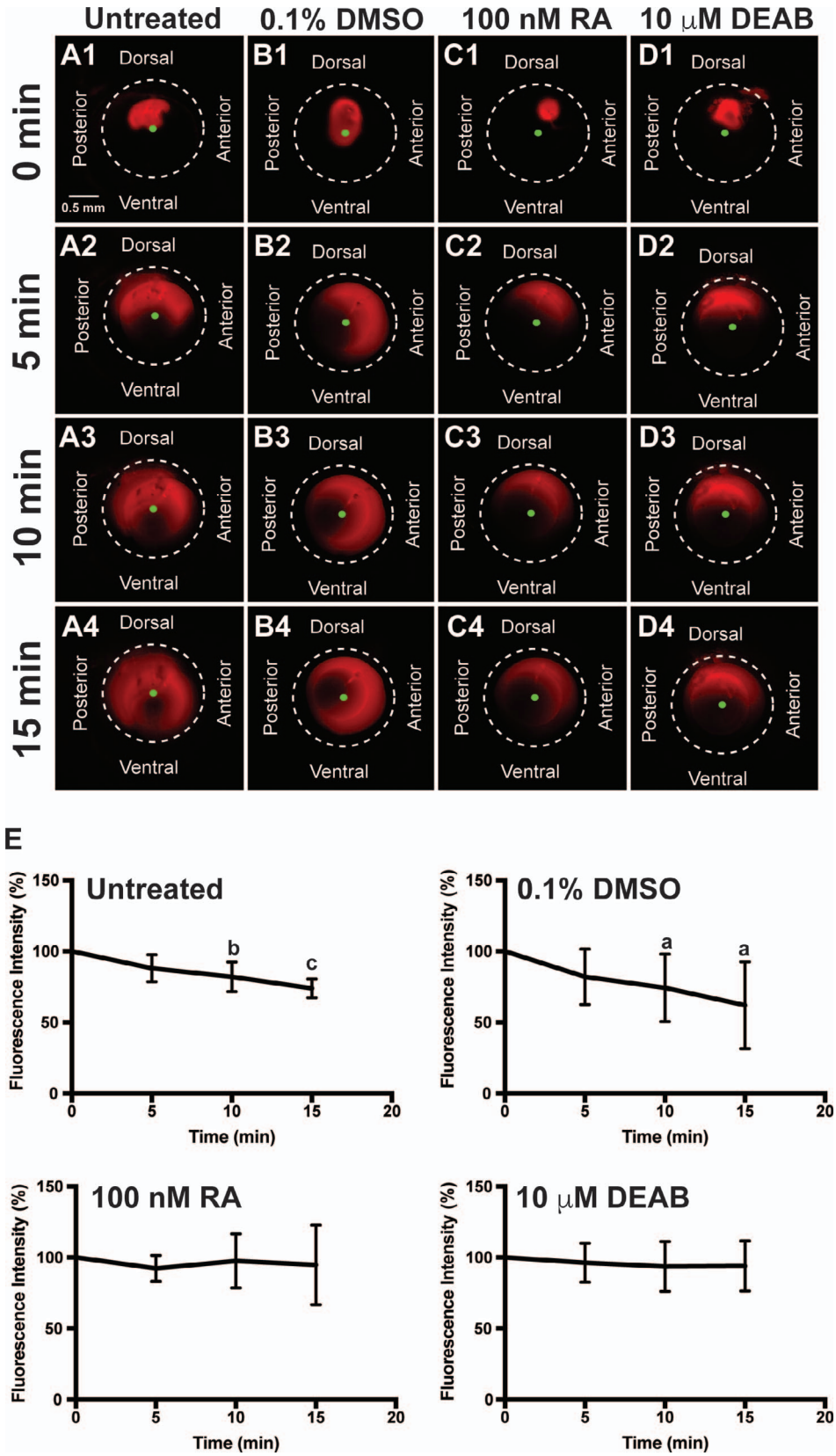

Figure 6. RA regulates aqueous outflow from the anterior segment of the eye. In vivo analysis of aqueous outflow showed that fluorescent Texas red dye injected into the anterior chamber diffused clockwise and counterclockwise toward the ventral iridocorneal angle over 15 minutes in untreated (**A1–A4**) fish. The fluorescence intensity of the dye did not change at 5 minutes (88.3% ± 9.6%), but was significantly decreased at 10 minutes (82.1% ± 10.4%) and 15 minutes (73.9% ± 6.7%) after injection (**E**). Similarly, the fluorescent dye diffused and exited the eye in fish treated for 2 days with 0.1% DMSO control (**B1–B4**). Fluorescence intensity was not changed at 5 minutes (81.8% ± 19.6%), but was significantly decreased

at 10 minutes (74.3% ± 23.8%) and 15 minutes (62.0% ± 30.5%) after injection in control-injected fish (**E**). Fish treated with 100 nM RA for 2 days showed initial diffusion of the dye (**C1**), but no significant decrease in dye intensity at 5 minutes (92.3% ± 9.1%; [**C2**]), 10 minutes (97.6% ± 19.0%; [**C3**]), and 15 minutes (94.9% ± 28.1%; [**C4**, **E**]). Fish treated with 10 μM DEAB for 2 days also demonstrated initial dye diffusion (**D1**), but no significant decrease in dye intensity at 5 minutes (96.3% ± 13.8%; [**D2**]), 10 minutes (93.7% ± 17.6%; [**D3**]), and 15 minutes (94.1% ± 17.6%; [**D4**, **E**]).

Exogenous RA treatment for 5 days increased RA activity within the IS and ventral canalicular network (Figs. 3C1, 3C2, arrows); however, activity with the retina (Fig. 3C3) and the overall fluorescence intensity within the eye did not show a significant change (25.5 ± 1.1; Fig. 4). Treatment with DEAB for 5 days decreased RA activity (Fig. 3D) and fluorescence intensity (16.5 ± 1.7) throughout the eye as compared to untreated ($P < 0.01$, Fig. 4) or DMSO control–treated ($P < 0.0001$; Fig. 4) fish. DEAB decreased RA activity in the RPE, PRs, OPL, IPL (Fig. 3D3), IS, and ventral canalicular network (Figs. 3D2, 3D3, arrows). Treatment with the RARα-specific antagonist BMS195614 (1 μM; Figs. 3E, 3E1, 3E2, 3E3) did not alter RA activity within the eye (24.4 ± 4.9; Fig. 4). Similarly, the RARβ-specific antagonist LE135 (1 μM; Figs. 3F, 3F1, 3F2, 3F3) did not decrease RA activity and overall fluorescence intensity within the eye (27.3 ± 3.1; Fig. 4). In contrast, the RARγ-specific antagonist MM11253 (10 nM) decreased RA activity (Figs. 3G, 3G1, 3G2, 3G3) and fluorescence intensity (11.9 ± 2.7; Fig. 4) throughout the eye as compared to untreated ($P < 0.01$) and DMSO control–treated ($P < 0.0001$) fish.

The effects of RA on ocular histology were further analyzed by using methylacrylate sections. Treatment with 100 nM RA for 5 days (Fig. 5C) decreased the cellular density of the corneal epithelium (Fig. 5C1, arrows) as compared to untreated (Figs. 5A, 5A1) and DMSO control–treated (Figs. 5B, 5B1) fish. In the ventral iridocorneal angle, the webbed annular ligament and ventral canalicular network were lost (Fig. 5C3, arrows), and decreased cellularity of the IS (Fig. 5C3) was observed as compared to untreated (Fig. 5A3) and DMSO control–treated (Fig. 5B3) fish. The dorsal iridocorneal angle (Fig. 5C2) and retina (Fig. 5C4) in RA-treated fish retained the same architecture observed in untreated (Figs. 5A2, 5A4) and 0.1% DMSO control–treated (Figs. 5B2, 5B4) fish. Treatment with DEAB (Fig. 5D) resulted in corneal epithelial (Fig. 5D1, arrows) and corneal stromal (Fig. 5D1, arrowheads) edema and loss of the cellularity and structure of the dorsal (Fig. 5D2) and ventral iridocorneal (Fig. 5D3) angles. Further, a loss of the structural architecture of the retina, including the obliteration of the PRs and ganglion cell layer, and decreased cellularity of the outer and inner nuclear layers, were observed (Fig. 5D4). Thus, tight control of RA levels was required for the maintenance of ocular structures, with increased RA levels specifically affecting the anterior segment, including the aqueous outflow tract structures.

RA Regulates Aqueous Humor Outflow From the Anterior Segment of Adult Eyes

Since exogenous RA and DEAB affected anterior segment anatomy and morphology, the effect of altering RA levels on aqueous outflow was analyzed in vivo. In untreated fish and fish treated with DMSO for 2 days, Texas Red fluorescent dye injected into the anterior chamber (Figs. 6A1, 6B1) diffused both clockwise and counterclockwise toward the ventral iridocorneal angle within the first 5 minutes (Figs. 6A2, 6B2; Supplementary Videos S6, S7). Between 5 and 15 minutes after injection, the dye decreased in intensity as it exited the anterior segment through the ventral canalicular network (Figs. 6A3, 6A4, 6B3, 6B4). In untreated and 0.1% DMSO control–treated fish, the fluorescence intensity (Fig. 6E) was not decreased after 5 minutes (88.3% ± 9.6%, 81.8% ± 19.6%), but was significantly decreased after 10 minutes (82.1% ± 10.4%, $P < 0.01$; 74.3% ± 23.8%, $P < 0.05$) and 15 minutes (73.9% ± 6.7%, $P < 0.001$; 62.0% ± 30.5%, $P < 0.05$). Following 2 days of exogenous RA (100 nM) treatment, the Texas Red dye initially diffused from the site of injection (Figs. 6C1, 6C2), but did not significantly decrease in intensity (92.3% ± 9.1% at 5 minutes, 97.6% ± 19.0% at 10 minutes, and 94.9% ± 28.1% at 15 minutes; Fig. 6E) throughout the duration of the experiment (Figs. 6C3, 6C4; Supplementary Video S8). Thus, RA decreased aqueous outflow from the anterior chamber. Similarly, in fish treated with DEAB (10 μM) for 2 days, the injected dye (Fig. 6D1) did not decrease in intensity at 5 minutes (96.3% ± 13.8%; Figs. 6E, 6D2), 10 minutes (93.7% ± 17.6%; Figs. 6E, 6D3), and 15 minutes (94.1% ± 17.6%; Figs. 6E, 6D4; Supplementary Video S9). These results showed that both increased or decreased RA levels decreased aqueous outflow from the anterior segment of the eye.

Tight Control of RA Is Required for Cell Survival in the Eye

The cellular and molecular effects of RA and DEAB within the adult eye were next analyzed by using a TUNEL assay and qRT-PCR. After 2 days of treatment, exogenous RA did not significantly increase the percentage of apoptotic cells throughout the adult eye (4.8% ± 7.3%; Fig. 7A) as compared to untreated (2.0% ± 2.4%,) and 0.1% DMSO control–treated (3.0% ± 3.5%) fish. However, localization of apoptotic cells showed that there was increased TUNEL staining in the IS and canalicular network in the ventral angle (Fig. 7D2) and the RPE (Fig. 7D3) as compared to untreated (Figs. 7B1, 7B2, 7B3) and 0.1% DMSO control–treated fish (Figs. 7C1, 7C2, 7C3). Treatment with RA did not affect cell survival in the dorsal iridocorneal angle (Fig. 7D1). Treatment with 10 μM DEAB for 2 days significantly increased the percentage of apoptotic cells in the eye (9.3% ± 5.4%, $P < 0.001$; Fig. 7A), including in both iridocorneal angles (Figs. 7E1, 7E2) and the retina (Fig. 7E3). The RARβ-specific antagonist BMS195614 (1 μM) did not affect cell survival (4.1% ± 4.8%; Fig. 7A) in the eye (Figs. 7F1, 7F2, 7F3) after 2 days of treatment. The RARβ-specific antagonist LE135 (1 μM) did not significantly increase the percentage of apoptotic cells in the eye (5.2% ± 4.6%; Figs. 7G1, 7G2, 7A), but did show apoptotsis in the photoreceptors and retinal pigment epithelium (Fig. 7G3) after 2 days. Treatment with the RARβ-specific antagonist MM11253 (10 nM) for 2 days did not significantly change the percentage of apoptotic cells in the eye (4.6% ± 6.2%; Figs. 7H1, 7A), but showed apoptosis in the retinal pigment epithelium (Fig. 7H3) and the IS in the ventral angle (Fig. 7H2). Quantitative RT-PCR demonstrated that treatment with 100 nM RA or 10 μM DEAB for 2 days did not significantly change the expression of the genes encoding RARα, RARβ, or RARγ (Supplementary Fig. S2). Further, RA or DEAB did not affect *myoc* or *pitx2a* expression within the adult eye. Thus, RA has localized effects on ocular cell survival, which appear to be predominantly mediated by RARβ and RARγ, but after 2 days of treatment did not significantly alter overall expression of RARs or downstream targets within the eye.

Investigative Ophthalmology & Visual Science

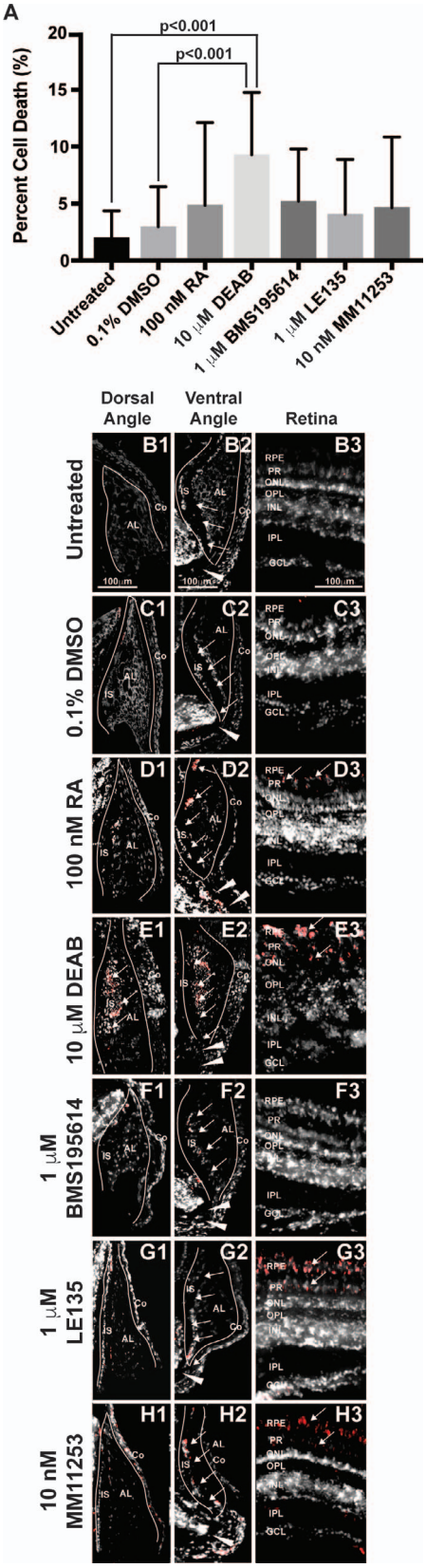

Figure 7. RA regulates cell survival in the anterior segment and retina. TUNEL assay showed that 2-day treatment with 10 μM DEAB (9.3% ± 5.4%) significantly increased the percentage of apoptotic cells (**A**) within the adult zebrafish eye as compared to untreated (2.0% ± 2.4%, $P < 0.001$) and 0.1% DMSO control–treated fish (3.0% ± 3.5%, $P < 0.001$). Two-day treatment with 100 nM RA (4.8% ± 7.3%), 1 μM BMS195614 (4.1% ± 4.8%), 1 μM LE135 (5.2% ± 4.6%), or 10 nM MM11253 (4.6% ± 6.2%) did not significantly change the percentage of apoptotic cells in the zebrafish eye. Despite no significant change in percentage of apoptotic cells in the eye, apoptosis was localized in RA-treated fish to the IS, canalicular network (*arrows*), and aqueous plexus (*arrowheads*) in the ventral iridocorneal angle (**D2**) as compared to untreated (**B2**) and DMSO control–treated (**C2**) fish. RA also showed increased apoptosis within the retinal pigment epithelium (*arrows*, [**D3** compared to **B3** and **C3**]), but did not affect cell survival in the dorsal iridocorneal angle (**D1** compared to **B1** and **C1**). Treatment with DEAB (10 μM) for 2 days caused diffuse apoptosis in the dorsal (**E1**) and ventral (**E2**) iridocorneal angles and in the retinal pigment epithelium and photoreceptors of the retina (*arrows*, [**E3**]). Treatment with the RARα-specific antagonist BMS195614 (1 μM) for 2 days did not affect cell survival in the dorsal angle (**F1**), ventral angle (**F2**), or the retina (**F3**). Inhibition of RARβ with LE135 (1 μM) for 2 days did not increase apoptosis in the angles (**G1**, **G2**) but did increase apoptosis in the retina (*arrows*, [**G3**]). The RARγ antagonist MM11253 (10 nM) caused localized apoptosis in the ventral angle (**H2**) and retina (**H3**), but not the dorsal angle (**H1**). AL, annular ligament; Co, cornea; GCL, ganglion cell layer; INL, inner nuclear layer; ONL, outer nuclear layer.

Discussion

Identifying the genes that regulate postnatal craniofacial and ocular structures is essential for understanding the pathogenesis of diseases that affect these tissues. The same signals that regulate cranial neural crest development may also play a role in the maintenance of structure and function in their adult-derived tissues. On the basis of this hypothesis, the present study examined the effect of RA on the craniofacial region and eye in adult zebrafish.

Previous studies have demonstrated that increased levels of RA in the postnatal craniofacial region alter the bone density of the mandible and skull.[34–36] The effects of hypervitaminosis A can result in damage to the mandible, showing perforations in rats and decreased skull thickness in mice. Additional studies have demonstrated that excess vitamin A increases bone turnover by decreasing osteoblast and increasing osteoclast activities.[34] These findings correlate with the skull defects observed in humans, zebrafish, and mice carrying null mutations in the *CYP26B1* gene.[37,38] In the present study, we further showed that RA regulates the dimensions of neural crest–derived craniofacial structures in the adult zebrafish. Exogenous treatment with or the decreased endogenous synthesis of RA affected jaw morphology or head height within 5 days, indicating the continuous regulation of RA levels within the adult craniofacial skeleton. In adult zebrafish, increased RA resulted in a prognathic jaw, which may reflect an imbalance between osteoblast and osteoclast activities. In contrast, the inhibition of RA synthesis decreased head height. While this effect might reflect changes in osteoblast and osteoclast activity, studies have shown that the decreased head height could also result from widespread cell death, as endogenous RA promotes cell survival.[39–42] Additional studies are required to determine the mechanisms by which endogenous RA maintains bone structure and inhibits apoptosis within the adult craniofacial region. Taken together, these studies demonstrated that the tight control of RA levels is critical for maintaining the structure and cell survival of the bony craniofacial structures in the adult.

In addition to the craniofacial bones and cartilage, the cranial neural crest contributes to the corneal stroma and endothelium, IS, sclera, and aqueous outflow tracts in the anterior segment of the eye. The formation of these structures is highly dependent on RA.[31,43,44] In the present study, we found that RA continued to play a role in neural crest–derived anterior segment structures as RA activity was localized to the adult zebrafish IS, ventral canalicular network, and angular

aqueous plexus. Notably, zebrafish do not have a trabecular meshwork like mice and humans, thus aqueous humor egresses from the anterior segment via the canalicular network, located between the IS and annular ligament in the ventral iridocorneal angle. The canalicular network subsequently drains into the angular aqueous plexus.[33,45]

We observed that both increased and decreased RA levels decreased cell survival, leading to subsequent histologic changes in the ventral iridocorneal angle and decreased aqueous outflow from the anterior chamber. Treatment with DEAB decreased cell survival throughout the eye, including the retina, cornea, and dorsal and ventral iridocorneal angles. As in the craniofacial region, this effect may reflect the need for endogenous RA for cell survival. Expectedly, loss of these ocular structures resulted in blindness and decreased aqueous outflow. In contrast, treatment with exogenous RA had a more specific effect on cell death within the ventral iridocorneal angle. Although tight control of endogenous RA levels is critical for cell survival, the increased apoptosis due to exogenous RA or DEAB may mask additional functions of RA within the eye. For example, RA regulates the collagen composition and alters the balance between different collagen α chains in various cell types.[46,47] In the ventral angle, the collagen distribution in the extracelular matrix may be influenced by endogenous RA levels, and increased or decreased RA may have subsequent effects on aqueous outflow that are hidden by apoptosis.[48] Additional studies examining the different functions of RA are required.

Previous studies have suggested potential targets of RA in the anterior segment. In cultured trabecular meshwork cells, RA regulates the expression of the trabecular meshwork inducible glucocorticoid response myocilin (*MYOC*) gene.[49] Mutations that decrease the secretion of MYOC protein are associated with juvenile and adult-onset primary open angle glaucoma.[50–52] Although we have previously observed that RA regulates *myoc* expression in cranial neural crest cells in zebrafish embryos (unpublished data), in the present study, we found that treatment with exogenous RA or inhibition of RA synthesis did not significantly change *myoc* expression in the adult eye. However, in zebrafish, *myoc* is also expressed in the retina and optic nerve.[53] Thus, the effect of RA on anterior segment expression of *myoc* may have been concealed by *myoc* expression in the posterior segment, which is independent of RA. A second potential target is the homeobox transcription factor *PITX2*. In humans, mutations in *PITX2* are associated with Axenfeld-Rieger syndrome, which is characterized by corneal, iris, and trabecular meshwork abnormalities.[54–56] During development, RA regulates the expression of *pitx2* in the periocular neural crest, such that ocular abnormalities due to RA deficiency can be rescued by *Pitx2*.[31,57] Similar to *myoc*, *pitx2* is also expressed in the adult zebrafish retina and this expression may have affected the qRT-PCR results in the present study. Additional studies identifying downstream targets of RA within the adult anterior segment are required. Nevertheless, these studies highlight the importance of the tight control of RA levels in adult tissues, as RA can have both pro- and antiapoptotic effects, depending on the biological system and concentration of this compound.

The maintenance of anterior segment structures is critical for visual function, as deterioration of these tissues characterizes blinding degenerative diseases. The identification of genes and signals that regulate aqueous outflow provide insight into the pathogenesis of primary open angle glaucoma. In the present study, we demonstrated a continued requirement for RA within the adult zebrafish anterior segment to maintain the structure and function of the aqueous outflow pathways.

Acknowledgments

The authors thank Mitchell Gillett and the Kellogg Eye Center Morphology and Imaging Module for technical assistance.

Supported by a Grant from the National Eye Institute of the National Institutes of Health (K08EY022912-01) and the Alcon Research Institute.

Disclosure: **B. Chawla**, None; **W. Swain**, None; **A.L. Williams**, None; **B.L. Bohnsack**, None

References

1. de la Cruz E, Sun S, Vangvanichyakorn K, Desposito F. Multiple congenital malformations associated with maternal isotretinoin therapy. *Pediatrics*. 1984;74:428–430.
2. Deltour L, Ang HL, Duester G. Ethanol inhibition of retinoic acid synthesis as a potential mechanism for fetal alcohol syndrome. *FASEB J*. 1996;10:1050–1057.
3. Rosa FW, Wilk AL, Felsey FO. Teratogen update: vitamin A congeners. *Teratology*. 1986;33:355–364.
4. Shean ML, Duester G. The role of alcohol dehydrogenase in retinoic acid homeostasis and fetal alcohol syndrome. *Alcohol Alcohol Suppl*. 1993;2:51–56.
5. Cunningham TJ, Duester G. Mechanisms of retinoic acid signalling and its roles in organ and limb development. *Nat Rev Mol Cell Biol*. 2015;16:110–123.
6. Das BC, Thapa P, Karki R, et al. Retinoic acid signaling pathways in development and diseases. *Bioorg Med Chem*. 2014;22:673–683.
7. Aldahmesh MA, Khan AO, Hijazi H, Alkuraya FS. Mutations in ALDH1A3 cause microphthalmia. *Clin Genet*. 2013;84:128–131.
8. Casey J, Kawaguchi R, Morrissey M, et al. First implication of STRA6 mutations in isolated anophthalmia, micropthalmia, and coloboma: a new dimension to the STRA6 phenotype. *Hum Mutation*. 2011;32:1417–1426.
9. Fares-Taie L, Gerber S, Chassing N, et al. ALDH1A3 mutations cause recessive anophthalmia and microphthalmia. *Am J Hum Genet*. 2013;92:265–270.
10. Golzio C, Martinovic-Bouriel J, Thomas S, et al. Matthew-Wood syndrome is caused by truncating mutations in the reitnol-binding protein receptor gene STRA6. *Am J Hum Genet*. 2007;80:1179–1187.
11. Pasutto F, Sticht H, Hammersen G, et al. Mutations in STRA6 cause a broad spectrum of malformations including anophthalmia, congenital heart defects, diaphragmatic hernia, alveolar capillary dysplasia, lung hypoplasia, and mental retardation. *Am J Hum Genet*. 2007;80:550–560.
12. Roos L, Fang M, Dali C, et al. A homozygous mutation in a consanguineous family consolidates the role of ALDH1A3 in autosomal recessive microphthalmia. *Clin Genet*. 2014;86:276–281.
13. Srour M, Chitayat D, Caron V, et al. Recessive and dominant mutations in retinoic acid receptor beta in cases with microphthalmia and diaphragmatic hernia. *Am J Hum Genet*. 2013;93:765–772.
14. Bohnsack BL, Kahana A. Thyroid hormone and retinoic acid interact to regulate zebrafish craniofacial neural crest development. *Dev Biol*. 2013;373:300–309.
15. Chawla B, Schley E, Williams AL, Bohnsack BL. Retinoic acid and *pitx2* regulate early neural crest survival and migration in craniofacial and ocular development. *Birth Defects Res B Dev Reprod Toxicol*. 2016;107:126–135.
16. Trainor PA, Tam PP. Cranial paraxial mesoderm and neural crest of the mouse embryo-codistribution in the craniofacial mesenchyme but distinct segreation in the branchial arches. *Development*. 1995;229:14–29.

17. Mayo-Wilson E, Imdad A, Herzer K, Yakoob MY, Bhutta ZA. Vitamin A supplements for preventing mortality, illness, and blindness in children aged under 5: systematic review and meta-analysis. *BMJ*. 2011;343:d5094.
18. West KPJ. Vitamin A deficiency disorders in children and women. *Food Nutr Bull*. 2003;24:S78–S90.
19. Barker ME, McCloskey E, Saha S, et al. Serum retinoids and beta-carotene as predictors of hip and other fractures in elderly women. *J Bone Miner Res*. 2005;20:913–920.
20. Maggio D, Polidori MD, Barabani M, et al. Low levels of carotenoids and retinol in involutional osteoporosis. *Bone*. 2006;38:244–248.
21. Melhus H, Michaëlsson K, Kindmark A, et al. Excessive dietary intake of vitamin A is associated with reduced bone mineral density and increased risk for hip fracture. *Ann Intern Med*. 1998;129:770–778.
22. Opotowsky AR, Bilezikian JP, NIf-u S. Serum vitamin A concentration and the risk of hip fracture among women 50 to 74 years old in the United States: a prospective analysis of the NHANES I follow-up study. *Am J Med Genet*. 2004;117: 169–174.
23. Promislow JH, Goodman-Gruen D, Slymen DJ, Barrett-Connor E. Retinol intake and bone mineral density in the elderly: the Rancho Bernardo Study. *J Bone Miner Res*. 2002;17:1349–1358.
24. Green AC, Martin TJ, Purton LE. The role of vitamin A and retinoic acid receptor signaling in post-natal maintenance of bone. *J Steroid Biochem Mol Biol*. 2016;155:135–146.
25. Blasiak RC, Stamey CR, Burkhart CN, Lugo-Somolinos A, Morrell DS. High-dose isotretinoin treatment and the rate of retrial, relapse, and adverse effects in patients with acne vulgaris. *JAMA Dermatol*. 2013;149:1392–1398.
26. Preneau S, Dessinioti C, Nguyen JM, Katsambas A, Dreno B. Predictive markers of response to isotretinoin in female acne. *Eur J Dermatol*. 2013;23:478–486.
27. Connolly RM, Nguyen NK, Sukumar S. Molecular pathways: current role and future directions of the retinoic acid pathway in cancer prevention and treatment. *Clin Cancer Res*. 2013; 19:1651–1659.
28. Siddikuzzaman C, Guruvayoorappan C, Berlin Grace VM. All trans retinoic acid and cancer. *Immunopharmacol Immunotoxicol*. 2011;33:241–249.
29. Bohnsack BL, Gallina D, Kahana A. Phenothiourea sensitizes zebrafish cranial neural crest and extraocular muscle develop-mnt to changes in retinoic acid and insulin-like growth factor signaling. *PLoS One*. 2011;6:e22991.
30. Bohnsack BL, Gallina D, Thompson H, et al. Development of extraocular muscles require early signals from periocular neural crest and the developing eye. *Arch Ophthalmol*. 2011; 129:1030–1041.
31. Bohnsack BL, Kasprick D, Kish PE, Goldman D, Kahana A. A zebrafish model of Axenfeld-Rieger Syndrome reveals that *pitx2* regulation by retinoic acid is essential for ocular and craniofacial development. *Invest Ophthalmol Vis Sci*. 2012; 53:7–22.
32. Williams AL, Eason J, Chawla B, Bohnsack BL. Cyp1b1 regulates ocular fissure closure through a retinoic acid-independent pathway. *Invest Ophthalmol Vis Sci*. 2017;58: 1084–1097.
33. Gray MP, Smith RS, Soules KA, John SWM, Link BA. The aqueous humor outflow pathway of zebrafish. *Invest Ophthalmol Vis Sci*. 2009;50:1515–1521.
34. Lind T, Öhman C, Calounova G, et al. Excessive dietary intake of vitamin A reduces skull bone thickness in mice. *PLoS One*. 2017;12:e0176217.
35. Barnicot N, Datta S. Vitamin A and bone. In: Bourne G, ed. *The Biochemistry and Physiology of Bone*. New York: Academic Press Inc; 1956:507–537.
36. Togari A, Kondo M, Arai M, Matsumoto S. Effects of retinoic acid on bone formation and resorption in cultured mouse calvaria. *Gen Pharmacol*. 1991;22:287–292.
37. Spoorendonk KM, Peterson-Maduro J, Renn J, et al. Retinoic acid and Cyp26b1 are critical regulators of osteogenesis in the axial skeleton. *Development*. 2008;135:3765–3774.
38. Laue K, Pogoda HM, Daniel PB, et al. Craniosynostosis and multiple skeletal anomalies in humans and zebrafish result from a defect in the localized degradation of retinoic acid. *Am J Hum Genet*. 2011;89:595–606.
39. Molina-Jijón E, Rodrííguez-Muñoz R, Namorado Mdel C, et al. All-trans retinoic acid prevents oxidative stress-induced loss of renal tight junction proteins in type-1 diabetic model. *J Nutr Biochem*. 2015;26:441–454.
40. Zhong C, Pu LY, Fang MM, Gu Z, Rao JH, Wang XH. Retinoic acid receptor alpha promotes autophagy to alleviate liver ischemia and reperfusion injury. *World J Gastroenterol*. 2015; 21:12381–12391.
41. Anguiano J, Garner TP, Mahalingam M, Das BC, Gavathiotis E, Cuervo AM. Chemical modulation of chaperone-mediated autophagy by retinoic acid derivatives. *Nat Chem Biol*. 2013; 9:374–382.
42. Crockett S, Clark M, Reeves S, Sims B. Cystine glutamate exchanger upregulation by retinoic acid induces neuroprotection in neural stem cells. *Neuroreport*. 2011;22:598–602.
43. Matt N, Dupe V, Garnier J-M, et al. Retinoic acid-dependent eye morphogenesis is orchestrated by neural crest cells. *Development*. 2005;132:4789–4800.
44. Matt N, Ghyselinck NB, Pellerin I, Dupe V. Impairing retinoic acid signalling in the neural crest cells is sufficient to alter entire eye morphogenesis. *Dev Biol*. 2008;320:140–148.
45. Soules KA, Link BA. Morphogenesis of the anterior segment in the zebrafish eye. *BMC Dev Biol*. 2005;5:12.
46. Kimura K, Zhou H, Orita T, Kobayashi M, Nishida T, Sonoda KH. Suppression by an RAR-gamma agonist of collagen degradation mediated by corneal fibroblasts. *Invest Ophthalmol Vis Sci*. 2017;58:2250–2257.
47. Kong R, Cui Y, Fisher GJ, et al. A comparative study of the effects of retinol and retinoic acid on histological, molecular, and clinical properties of human skin. *J Cosmet Dermatol*. 2016;15:49–57.
48. De Groef L, Andries L, Siwakoti A, et al. Aberrant collagen composition of the trabecular meshwork results in reduced aqueous humor drainage and elevated IOP in MMP-9 null mice. *Invest Ophthalmol Vis Sci*. 2016;57:5984–5995.
49. Prat C, Belville C, Comptour A, et al. Myocilin expression is regulated by retinoic acid in the trabecular meshwork-derived cellular environment. *Exp Eye Res*. 2017;155:91–98.
50. Mimivati Z, Nurliza K, Marini M, Liza-Sharmini A. Identification of MYOC gene mutation and polymorphism in a large Malay family with juvenile-onset open angle glaucoma. *Mol Vis*. 2014;20:714–723.
51. Kuchtey J, Chowdhury UR, Uptegraft CC, Fautsch MP, Kuchtey RW. A de novo MYOC mutation detected in juvenile open angle glaucoma associated with reduced myocilin protein in aqueous humor. *Eur J Med Genet*. 2013;56:292–296.
52. Angius A, Spinelli P, Ghilotti G, et al. Myocilin Gln368stop mutation and advanced age as risk factors for late-onset primary open-angle glaucoma. *Arch Ophthalmol*. 2000;118: 674–679.
53. McMahon C, Semina EV, Link BA. Using zebrafish to study the complex genetics of glaucoma. *Comp Biochem Physiol C Toxicol Pharmacol*. 2004;138:343–350.
54. Ozeki H, Shirai S, Ikeda K, Ogura Y. Anomalies associated with Axenfeld-Rieger syndrome. *Graefes Arch Clin Exp Ophthalmol*. 1999;237:730–734.

Investigative Ophthalmology & Visual Science

55. Strungaru MH, Dinu I, Walter MA. Genotype-phenotype correlations in Axenfeld-Rieger malformation and glaucoma patients with FOXC1 and PITX2 mutations. *Invest Ophthalmol Vis Sci*. 2007;48:228–237.
56. Tumer Z, Bach-Holm D. Axenfeld-Rieger syndrome and spectrum of Pitx2 and Foxc1 mutations. *Eur J Hum Genet*. 2009;17:1527–1539.
57. Kumar S, Duester G. Retinoic acid signaling in perioptic mesenchyme represses Wnt signaling via induction of Pitx2 and Dkk2. *Dev Biol*. 2010;340:67–74.

Supplementary Material

Supplementary Video S1. Optokinetic reflex in adult fish before treatment. Dorsal view of fish before initiation of treatment showed an intact optokinetic reflex that responds accurately to the drum, including changes of direction and pauses in movement.

Supplementary Video S2. Optokinetic reflex in untreated adult fish. Dorsal view of untreated fish showed that optokinetic reflexes were not disrupted by 5 days of dark conditions and fasting.

Supplementary Video S3. Optokinetic reflex in fish treated with 0.1% DMSO for 5 days. Treatment with 0.1% DMSO for 5 days did not inhibit visual behavior as exhibited by accurate optokinetic reflexes.

Supplementary Video S4. Optokinetic reflex in fish treated with 100 nM RA for 5 days. Fish treated with 100 nM RA for 5 days showed difficulty in changing direction with the optokinetic drum.

Supplementary Video S5. Optokinetic reflex in fish treated with 10 μM DEAB. Treatment with 10 μM DEAB for 5 days caused loss of visual function, as the eyes did not track the optokinetic drum.

Supplementary Video S6. In vivo aqueous outflow assay in untreated adult fish. Time-lapse movie of images taken every 20 seconds for 15 minutes following injection of Texas Red fluorescent dye in untreated adult zebrafish showed that the dye diffused throughout the anterior chamber and migrated clockwise and counterclockwise toward the ventral iridocorneal angle.

Supplementary Video S7. In vivo aqueous outflow assay in fish treated with 0.1% DMSO for 2 days. Time-lapse movie of images taken every 20 seconds for 15 minutes following injection of Texas Red fluorescent dye in an adult zebrafish treated with 0.1% DMSO for 2 days showed similar aqueous outflow pattern as untreated fish. The injected dye diffused throughout the anterior chamber and migrated clockwise and counterclockwise toward the ventral iridocorneal angle.

Supplementary Video S8. In vivo aqueous outflow assay in fish treated with 100 nM RA for 2 days. Time-lapse movie of images taken every 20 seconds for 15 minutes following injection of Texas Red fluorescent dye in an adult zebrafish treated with 100 nM RA for 2 days showed that the dye did not flow out of the anterior chamber. The injected dye initially dispersed around the site of injection, but subsequently did not diffuse throughout the anterior chamber or migrate toward the ventral iridocorneal angle.

Supplementary Video S9. In vivo aqueous outflow assay in fish treated with 10 μM DEAB for 2 days. Time-lapse movie of images taken every 20 seconds for 15 minutes following injection of Texas Red fluorescent dye in an adult zebrafish treated with 10 μM DEAB for 2 days showed that the dye did not flow out of the anterior chamber. The injected dye initially dispersed around the site of injection, but subsequently did not diffuse throughout the anterior chamber or migrate toward the ventral iridocorneal angle.

Investigative Ophthalmology & Visual Science